Renewable and Sustainable Energy Reviews 26 (2013) 752–760

Contents lists available at SciVerse ScienceDirect

Renewable and Sustainable Energy Reviews

journal homepage: www.elsevier.com/locate/rser

Models for the electrical characterization of high concentration photovoltaic cells and modules: A review

P. Rodrigo [a,*], E.F. Fernández [a], F. Almonacid [b], P.J. Pérez-Higueras [b]

[a] Center of Advanced Studies in Energy and Environment—Jaén University, Las Lagunillas Campus, C6 building, 23071 Jaén, Spain
[b] Electronic Engineering and Automatic Department–Jaén University, Las Lagunillas Campus, A3 Building, 23071 Jaén, Spain

ARTICLE INFO

Article history:
Received 15 February 2013
Received in revised form
14 June 2013
Accepted 16 June 2013
Available online 13 July 2013

Keywords:
Concentration photovoltaics
Cell model
Module model

ABSTRACT

High concentration photovoltaic technology promises the large-scale generation of clean-renewable energy with competitive costs. Like any other systems for electricity generation, it is important to know the electrical characteristics of the system. However, while there is a wide experience in modeling the behavior of traditional photovoltaic systems, not every model for flat-plate solar cells or modules is directly applicable to high concentration photovoltaic cells or modules because of the special features of these devices (use of multijunction cells, use of optics for high concentration, etc.). So, in recent years, the scientific community has devoted considerable efforts in developing models that reproduce the electrical behavior of high concentration cells and modules. These models allow calculating the main electrical parameters of the device from its operating conditions (irradiance, cell temperature, spectral distribution of the radiation, etc.). In this paper, a comprehensive review of existing models for the electrical characterization of high concentration photovoltaic cells and modules is presented with the aim of helping the photovoltaic professionals and researchers in the design, monitoring and energy prediction tasks.

Contents

Abbreviations: HCPV, High concentration photovoltaic; SOE, Secondary optical element; SEM, Single exponential model; DEM, Double exponential model; ESR, External spectral response.

* Corresponding author. Tel.: +34953213518; fax: +34953212183.
E-mail address: prodrigo@ujaen.es (P. Rodrigo).

1364-0321/$ - see front matter
http://dx.doi.org/10.1016/j.rser.2013.06.019

1. Introduction

High Concentration PhotoVoltaic (HCPV) cells and modules operate under concentration ratios between 300 and 2000 suns. The concentration mechanism is done by lenses or mirrors that either reflect or refract the sunlight on the solar cell surface. Replacing the expensive solar cell materials by cheaper optics offers the opportunity of reducing the costs of the modules. In addition, the use of multijunction solar cells implies an increase of the system efficiency, what also can reduce the associated costs [1].

Three main elements are required in order to generate electricity: the multijunction solar cell, the optics and the solar tracker. These elements can be combined in a lot of different configurations [2,3]. A typical commercial HCPV system is composed of concentration modules mounted on two-axis solar trackers, where each module contains several multijunction solar cells and each cell has its own optics, typically a point-focus Fresnel lens. Triple-junction GaInP/GaInAs/Ge cells are usually utilized [4], while other material combinations are now under research [5–8]. Other auxiliary elements are used, such as heat sinks, Secondary Optical Elements (SOEs), bypass diodes and protection elements. Nowadays, these configurations dominate the HCPV market and are very promising solutions for the future of photovoltaics [9].

Modeling the electrical behavior of HCPV cells and modules is an important task for the design, monitoring and energy prediction of these kinds of systems. In this paper, a review of the state-of-the-art of models that reproduce the operation of HCPV cells and modules is presented. These models calculate the I–V characteristic curve of the device from its operating conditions. Not every model allows calculating the whole I–V curve; some of them only calculate some relevant electrical parameters, such as the maximum power (P_{MPP}), the short-circuit current (I_{SC}), the open-circuit voltage (V_{OC}), the fill factor (FF), etc.

The presented models differ in the parameters required to characterize the device, in the variables used as inputs and, finally, in the equations and procedures used to obtain the electrical characteristics. The models present different levels of complexity and accuracy and require different equipments to be applied. This review remarks the characteristics of each one of these models in order to help in the choice of the most suitable model for each specific application.

The paper is organized as follows: in the second section, a brief overview of the technologies under study is presented; in the third section, the existing models for multijunction solar cells are summarized; the fourth section describes the main contributions in the modeling of HCPV modules; finally, section five comments the conclusions of the work.

2. Brief technology overview

The main elements that constitute a HCPV generator are the solar cells, the receivers, the optical devices and the tracking system. A collection of solar receivers with electrically interconnected cells and with integrated optical devices is known as a HCPV module. Next, the main characteristics of these elements are described.

2.1. Solar cells

High concentration solar cells have specific characteristics different to those of conventional flat-plate solar cells. The HCPV cells are designed to extract more energy under a larger solar radiation. These cells have to be exclusively made of high quality semiconductor materials because of the significance of the conversion efficiency, a factor which is directly related to the quality of the crystal used, in which impurities must be avoided.

An important characteristic of these solar cells is their enhanced thermal behavior. Under high temperatures, both Si and GaAs cells suffer a significant decrease of performance mainly because of the voltage reduction produced by a temperature increase. Nonetheless, this effect is less accurate at high concentration levels.

Despite the fact that many different types of cells are being tested at laboratory level and although the reported efficiency has increased over 40% for multijunction cells [10], many of the concentration systems installed nowadays use silicon solar cells, providing efficiencies which hardly exceed 25% under concentration. However, most of the current developments are based on triple-junction cells. These cells can be described as a stack of cells of different compositions with a progressively decreasing bandgap, so that the cell on the top of the stack absorbs higher energy photons than the cell in the middle, and this absorbs higher energy photons than the cell in the bottom.

2.2. Receivers

Solar cells have to be mounted on a receiver to extract the generated current and to dissipate and remove the heat resulting from sun power. Current extraction is made by thick wires or ribbons that are soldered to the cells, whereas heat removal is carried out by a heat sink added to the receiver. Materials like copper or aluminum are currently used for heat evacuation. Also, the solar receivers often include a bypass diode connected in parallel with the cell in order to avoid overheating of the cell in non-usual operating conditions such as shading.

2.3. Optical devices

The aim of the optical devices used in this technology is to concentrate radiation and to increase the luminous flux on the cells. Optical devices may be simple or consisting of primary and secondary optical element (SOE). Primary optical devices collect direct sun rays. Secondary optical devices receive the light from the primary ones and then change its properties by means of spectral filtering, light homogenization or light direction changing. In this respect, different optical devices are currently used: circular parabolic dishes, parabolic dishes with secondary, square flat Fresnel lenses, square flat Fresnel lenses with secondary, linear flat lenses, linear arched lenses or linear parabolic reflectors.

Most of the systems currently designed are based on Fresnel lenses. This kind of lens reduces the amount of material required to concentrate the light by splitting the lens into a set of concentric annular sections known as Fresnel zones. The use of these zones allows keeping the required curvature without increasing the

thickness by means of adding discontinuities between them. Fig. 1 shows an example of a solar receiver integrated with point-focus Fresnel lens.

2.4. HCPV module

A HCPV module is the smallest, complete, environmentally protected assembly of receivers and optical devices that is able to transform an input of unconcentrated solar radiation. Consequently, a typical HCPV module is made up of a group of cells, primary optics, secondary optics (optional) and housing components such as interconnection and mounting. Fig. 2 shows an example of a typical HCPV module and its components.

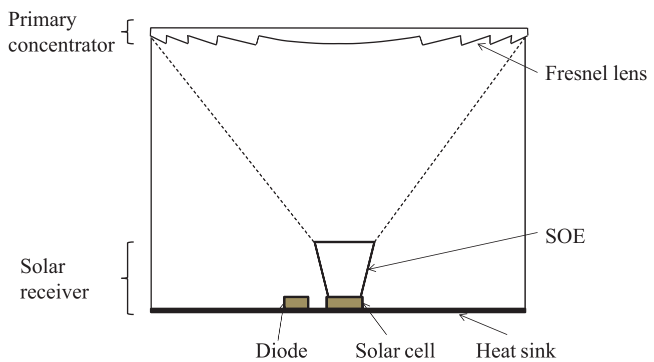


Fig. 1. Schematic of a HCPV solar receiver integrated with point-focus Fresnel lens.

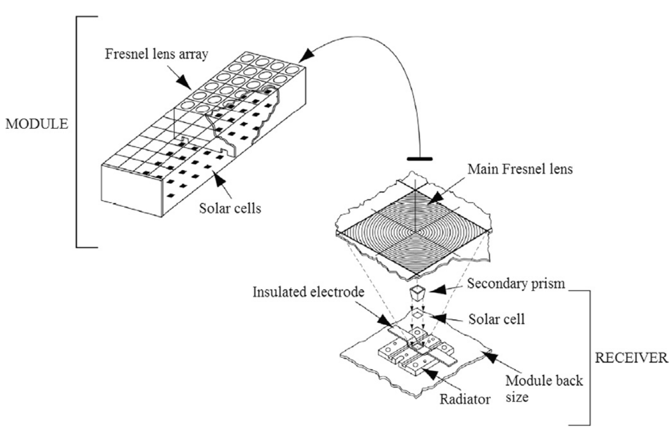


Fig. 2. Schematic of a HCPV module based on point-focus Fresnel lenses. *Source*: IEC 62108 [2].

2.5. Tracking system

Point-focus based HCPV modules must be always mounted on two-axis solar trackers, i.e. the modules must be always pointing the solar rays in order for the lenses to be able to focus the radiation on the small solar cell area. This kind of tracking system is more complex than linear tracking or static systems from a mechanical point of view but it presents the advantage of maximizing the solar radiation capture along the daily trajectory.

3. HCPV cells models

In this section, five existing models that reproduce the behavior of a multijunction solar cell operating under high concentration are summarized. The presented models assume certain simplifications in order to be applicable in engineering studies. Other more sophisticated models that divide the cell into hundreds or thousands of elementary cells are not included in this review [11,12]. These distributed models are difficult to implement and require high computational effort, so that they are not commonly used at the engineering level.

3.1. Models based on the equivalent circuit of the multijunction cell

A triple junction solar cell can be considered as composed of three series-connected p–n junctions. Each junction can be represented by an equivalent circuit model, being the most used models the Single Exponential Model (SEM) and the Double Exponential Model (DEM). Both models differ in the number of diodes that characterize the saturation current. By connecting the three subcells circuits in series, the equivalent circuit for the triple junction cell is obtained, Fig. 3.

Taking into account the DEM model, the cell *I–V* curve can be mathematically expressed by the next set of equations

$$V=\sum_{i=1}^{3} V_i \tag{1}$$

$$I=I_{PH,i}-I_{01,i}\{\exp[(V_i+IR_{S,i})/m_{1,i}V_T]-1\}\\ -I_{02,i}\{\exp[(V_i+IR_{S,i})/m_{2,i}V_T]\\ -1\}-(V_i+IR_{S,i})/R_{P,i}\ ,\ i=1,\ 2,\ 3 \tag{2}$$

where the subscript i indicates the subcell (1 = top, 2 = middle, 3 = bottom). Each subcell is characterized by a set of

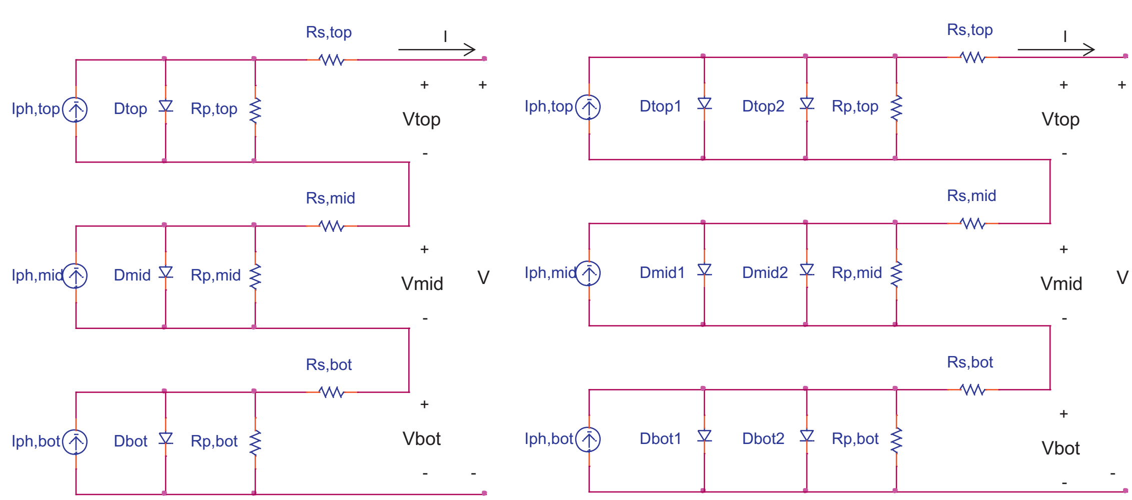


Fig. 3. Equivalent circuit models for triple junction solar cells by using the Single Exponential Model (left) and the Double Exponential Model (right).

7 parameters: $I_{PH,i}$ (the photocurrent), $I_{01,i}$ and $I_{02,i}$ (the saturation currents), $m_{1,i}$ and $m_{2,i}$ (the diode ideality factors), $R_{S,i}$ (the series resistance) and $R_{P,i}$ (the shunt resistance). V_T is the semiconductor thermal voltage, V_T=kT/q, being k the Boltzmann constant, T the absolute temperature of the junction and q the electron charge.

The equations for the SEM scheme are as follows:

$$V = \sum_{i=1}^{3} V_i \tag{3}$$

$$I = I_{PH,i} - I_{0,i}\{\exp[(V_i + IR_{S,i})/m_i V_T] - 1\} - (V_i + IR_{S,i})/R_{P,i}\ ,\ i = 1,\ 2,\ 3 \tag{4}$$

where each subcell is now characterized by 5 parameters: $I_{PH,i}$ (the photocurrent), $I_{0,i}$ (the saturation current), m_i (the diode ideality factor), $R_{S,i}$ (the series resistance) and $R_{P,i}$ (the shunt resistance).

In general, the model parameters depend on the operating conditions of the multijunction cell, such as concentration and cell temperature. However, as multijunction cells are often monolithic devices which incorporate only two electrical terminals, the separate measurement of the individual subcells is not possible. Therefore, the determination of the subcells parameters is very difficult.

Some authors have proposed methods for extracting the subcells parameters, or at least some of them, by applying different assumptions and simplifications. We can find several extraction methods based on both the SEM scheme [13–18] and the DEM scheme [17,19–23]. However, it is remarkable that these studies often estimate parameters only at particular operating conditions and not for the whole range of possible conditions, so that the application of these models is sometimes limited.

3.2. Model of G.S. Kinsey et al. (2008)

The model proposed by G.S. Kinsey et al. [24,25] allows calculating the maximum power (P_{MPP}) of a triple junction solar cell from its operating conditions: concentration ratio, X, cell temperature, T_C, and incident spectrum, $E(\lambda)$. First, three electrical parameters of the solar cell as a whole are calculated: the open-circuit voltage, V_{OC}, the fill factor, FF, and the short-circuit current density, J_{SC}. Once these parameters have been determined, the P_{MPP} is obtained by:

$$P_{MPP} = \mathrm{FF} J_{SC} A_{CEL} V_{OC} \tag{5}$$

A_{CEL} being the solar cell active area.

The V_{OC} and FF are assumed to be independent of the incident spectrum. While this assumption is adequate for the V_{OC} [26,27], the FF variations with spectrum can have a significant impact on performance [28,29]. However, in this model, these variations are neglected. The V_{OC} is obtained from the reference V_{OC} at one sun and 25 °C of cell temperature by applying a logarithmic correction with concentration and a linear correction with temperature. On the other hand, the FF is obtained from the reference FF by only applying a linear correction with temperature.

The model requires knowing the External Spectral Response of the component subcells (ESR_i) as a function of the wavelength, λ, at different cell temperatures. These functions must be measured with the help of a solar simulator. A solar simulator usually consists of three major components: (1) light source(s) and associated power supply; (2) any optics and filters required to modify the output beam and (3) the necessary controls to operate the simulator, adjust irradiance, etc. [30].

The model equations for calculating the short-circuit current density are:

$$J_{PHtop} = \int \mathrm{ESR}_{top}(\lambda, T_C) E(\lambda) d\lambda \tag{6}$$

$$J_{PHmid} = \int \mathrm{ESR}_{mid}(\lambda, T_C) E(\lambda) d\lambda \tag{7}$$

$$J_{SC} = \min\{J_{PHtop}, J_{PHmid}\} \tag{8}$$

where J_{PHtop}, J_{PHmid} are the photocurrents of the top and the middle subcells. Eq. (8) considers that the short-circuit current of the cell is limited by the smaller photocurrent of the top and middle subcells, i.e. the bottom subcell never limits the current.

The model requires knowing several parameters that characterize the multijunction cell, being the most important the ESR of the top and the middle subcells. These values are obtained with the help of the HIPSS solar simulator from Spectrolab [31]. In addition, the use of a spectroradiometer is required to measure the incident spectrum. Alternatively, the spectrum can be estimated from atmospheric parameters by using simulation software such as SMARTS [32,33].

3.3. Model of C. Domínguez et al. (2010)

The direct measurement of the spectrum is difficult and requires the use of a spectroradiometer, which is not always available. Another option is to use isotype cells. These sensors have the same spectral response than the component subcells of the multijunction device. This way, the photocurrents measured by the isotype cells under the same spectrum than the multijunction cell allow knowing the photocurrents of the component subcells.

The model proposed by C. Domínguez et al. [16] is based on the use of isotype cells. It is a translation model, which calculates the points of the I–V curve at the desired operating condition from the points of the I–V curve at the reference condition. Three translations are applied to each point of the reference I–V curve: (1) a translation of the current coordinate to the desired value of concentration; (2) a translation of the voltage coordinate to the desired values of concentration and incident spectrum; (3) a correction of the voltage coordinate to take into account the change in the cell operating temperature. This way, the model calculates the I–V characteristics as a function of irradiance, spectrum and cell temperature.

Translation equations are analytically obtained by considering the SEM equivalent circuit model for multijunction cells (Fig. 3). In this scheme, the three shunt conductances are neglected and the three series resistances are lumped into a single effective series resistance, R_S. For instance, the translation of the voltage coordinate due to the change in concentration and spectrum is represented by the following equation

$$V(T_{Cref}) = V_{ref} + \frac{k(T_{Cref} + 273.15)}{q} \left\{ m_{MJ} \ln(X) + \ln\left[\left(\frac{F_{top} I_{PHtop,ref} - I_{ref}}{I_{PHtop,ref} - I_{ref}} \right)^{mtop} \left(\frac{F_{mid} I_{PHmid,ref} - I_{ref}}{I_{PHmid,ref} - I_{ref}} \right)^{mmid} \left(\frac{F_{bot} I_{PHbot,ref} - I_{ref}}{I_{PHbot,ref} - I_{ref}} \right)^{mbot} \right] \right\} - I_{ref}(X-1)R_S \tag{9}$$

(V_{ref}, I_{ref}) being the considered point of the reference I–V curve, $V(T_{Cref})$ the translated voltage, $I_{PHi,ref}$ the photocurrents of the component subcells at reference conditions, X the desired concentration, m_i the diode ideality factors of the component subcells and m_{MJ} an effective ideality factor for the multijunction device. The factors F_i are defined for each subcell as

$$F_i = \frac{I_{PHi}/I_{PHi,ref}}{\min\{I_{PHtop}, I_{PHmid}, I_{PHbot}\}/\min\{I_{PHtop,ref}, I_{PHmid,ref}, I_{PHbot,ref}\}} \tag{10}$$

i.e. they account for the photocurrents of the subcells, $I_{PHi,}$ as measured by the isotype cells.

The model depends on some parameters that characterize the multijunction device. Some of them can be found in semiconductor textbooks but some other must be fitted by using simulation tools that minimize the error between experimental data and modeled data. A solar simulator is required to obtain the experimental data.

3.4. Model of E.F. Fernández et al. (2013)

The aim of the model proposed by E.F. Fernández et al. [34,35] is to obtain a model based on easily adjustable parameters.

The measurements of several multijunction cells showed that the Ge bottom subcell never limits the short-circuit current of the multijunction device and has a small influence on the rest of the electrical parameters under normal operating conditions. Therefore, the behavior of the cell can be modeled by considering only two "equivalent subcells" that verify the equation of the SEM model.

The short-circuit currents of the two equivalent subcells (I_{SC1}, I_{SC2}) are supposed to be equal than the photocurrents of the top and the middle real subcells. These photocurrents must be measured with isotype cells or calculated from the incident spectrum as measured by a spectroradiometer if the ESR of the subcells is known.

On the other hand, the open-circuit voltages of the equivalent cells (V_{OC1}, V_{OC2}) verify the condition that their sum is equal to the open-circuit voltage of the real cell. A logarithmic correction on concentration is used to calculate these open-circuit voltages from the V_{OC} values at one sun. The objective of calculating these open-circuit voltages is to obtain the saturation currents of the equivalent cells (I_{01}, I_{02}), which are computed by using well-known simplified expressions derived from the SEM solar cell model.

The equation of the *I–V* curve of the multijunction cell is modeled by means of a series association of the two equivalent subcells, i.e. the voltages of these subcells are summed in order to obtain:

$$V = \frac{\mathrm{mk}(T_C + 273.15)}{q}\left[\ln\left(\frac{I_{SC1} - I}{I_{01}}\right) + \ln\left(\frac{I_{SC2} - I}{I_{02}}\right)\right] - IR_S \tag{11}$$

R_S and m being effective values for the series resistance and the diode ideality factor of the multijunction device. Finally, this *I–V* curve is corrected taking into account an effective shunt resistance R_P.

Because of the simplicity of the model equations, the implementation of the numerical algorithm for obtaining the model parameters is easy. However, like in the models commented above, a set of measurements carried out in a solar simulator is required for adjusting these parameters.

3.5. Model of Sandia National Laboratories (2004)

The models commented above cannot always be applied in practice, because of the need of a solar simulator, the need of instruments such as spectroradiometer or isotype cells or the difficulty of implementing the algorithms for adjusting the model parameters. So, in some cases, the use of a simpler model could be justified in spite of a little loss in accuracy. The model developed at Sandia National Laboratories [36] was mainly conceived for characterizing modules and arrays of different technologies, but it also can be applied to high concentration solar cells. It does not require sophisticated instruments and the model parameters can be obtained from outdoor measurements.

As it has been shown, the main problem for characterizing multijunction cells is that they are very sensitive to the incident spectrum. In general, the sunlight spectrum varies as a function of air mass, clouds, turbidity due to aerosol effects and precipitable water vapor [28]. However, the main contribution to the spectrum change is air mass [37,38]. In the model of Sandia National Laboratories, the measurement of the sunlight spectrum is not required and the spectral influences are only quantified by the air mass parameter, as defined in [39].

The model equations are formulated as a function of the "effective irradiance" (B_{ef}). In the case of high concentration cells, this parameter is defined as:

$$B_{ef} = [G_B f_1(AM)]/G_B^* \tag{12}$$

G_B being the incident direct irradiance and G_B^* the reference direct irradiance. f_1(AM) is the spectral correction factor as defined in the standard ASTM E 973 [40], which is approximated by a fourth order polynomial function of the air mass.

Five points of the cell *I–V* curve are calculated by the model: the three classical points (short-circuit, open-circuit and maximum power points) and two additional points: (V_X, I_X), the point at a voltage $V_X = V_{OC}/2$, and (V_{XX}, I_{XX}), the point at a voltage $V_{XX} = (V_{MPP} + V_{OC})/2$. Fig. 4 indicates the position of these points on the cell *I–V* curve. As an example of the model equations, the expressions that allow calculating the I_{SC} and V_{OC} parameters are the following

$$I_{SC} = B_{ef}[I_{SC}^* + \alpha_{Isc}(T_C - T_C^*)] \tag{13}$$

$$V_{OC} = V_{OC}^* + \delta \ln(B_{ef}) + \beta_{Voc}(T_C - T_C^*) \tag{14}$$

where the superscript "*" indicates parameters at reference conditions. In these equations, the influence of cell temperature is modeled with the temperature coefficients α_{Isc} and β_{Voc}, where β_{Voc} is allowed to vary linearly with the effective irradiance. Coefficient δ is the product of the effective diode ideality factor, m, and the thermal voltage V_T.

Every model parameter can be obtained by regression analysis from outdoor monitorized data, what is an advantage with respect to other models. The main disadvantage of this model is that it does not take into account ambient factors that affect the sunlight spectrum, such as clouds, aerosols and precipitable water vapor. The model is oriented to clear days with clean atmosphere. However, it is remarkable that these conditions are prevalent at the locations where HCPV systems are installed.

Table 1 summarizes the main characteristics of the referenced models for high concentration photovoltaic cells, including the required inputs and advantages of each one.

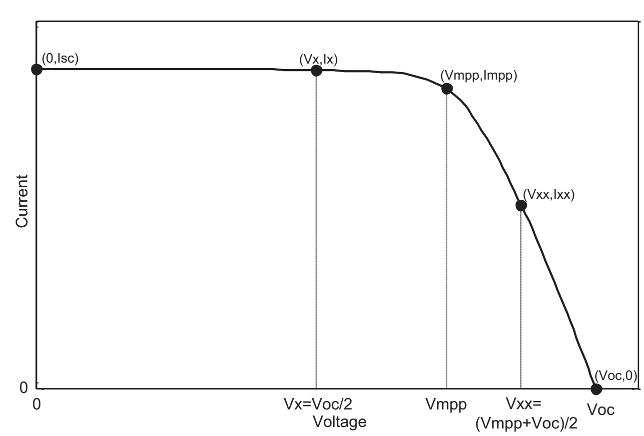


Fig. 4. Points of the *I–V* curve calculated by the model of Sandia National Laboratories.

4. Models for estimating the maximum power of a HCPV module

This section summarizes the state-of-the-art of models for HCPV modules characterization. These models take into account different atmospheric parameters that affect the behavior of the module, such as direct normal irradiance (DNI), air mass (AM), air temperature (T_{air}), wind speed (WS), etc., and some of the models use the mean cell temperature of the module (T_C) as input.

4.1. Model of the standard ASTM E 2527

The standard ASTM E 2527 [41] defines a very simple way of estimating the P_{MPP} of a high concentration module. It uses as inputs the direct normal irradiance (DNI), the air temperature (T_{air}) and the wind speed (WS). It is based on a single equation:

$$P_{MPP} = \mathrm{DNI}(c_1 + c_2\mathrm{DNI} + c_3 T_{air} + c_4\mathrm{WS}) \quad (15)$$

where c_1, c_2, c_3 and c_4 coefficients are obtained by regression analysis of outdoor monitorized data. As can be seen, the model does not take into account the spectral effects that significantly affect the behavior of modules containing multijunction solar cells.

4.2. Model of G. Peharz et al. (2011)

The model of G. Peharz et al. [42] does take into account the spectral influences. It is based on the following equation:

$$P_{MPP} = c_{DNI}\mathrm{DNI} + c_{Z2}Z^2 + c_Z Z + c_{Tc}T_C + c_{offset} \quad (16)$$

where the Z parameter represents the mismatch between the photocurrents of the top and middle subcells with respect to the reference AM1.5d spectrum. The value of Z is obtained from the photocurrents as measured by isotype cells [43]. A value of $Z > 0$ corresponds to a blue spectrum, where the limiting subcell is the middle subcell, while a value of $Z < 0$ corresponds to a red spectrum, where the limiting subcell is the top subcell. In order to quantify the value of Z, some parameters of the solar cell must be measured in a solar simulator. c_{DNI}, c_{Z2}, c_Z, c_{Tc} and c_{offset} coefficients are obtained by regression analysis from outdoor monitorized data.

4.3. Model of M. Steiner et al. (2012)

The model proposed by M. Steiner et al. [44] is a complete model that combines the spectrum simulation software SMARTS [32,33] with ray tracing software for modeling the optics of the Fresnel lenses [45] and a SPICE network model for modeling the *I–V* characteristics [46,47]. The model requires a complete set of instruments in order to be applied because it takes into account many factors that affect the module behavior. Beyond a pyrheliometer and weather station equipment, it requires isotype cells in order to measure the Z parameter, multifilter rotating shadowband radiometer for the determination of Aerosol Optical Depth (AOD) and Precipitable Water (PW) and tracking accuracy sensor for measuring the alignment of the tracker to the sun. The model allows calculating the P_{MPP} of high concentration modules with a high level of accuracy, being its main disadvantages the difficulty of implementing and the equipment requirements.

4.4. Model of A.J. Rivera et al. (2013)

Due to the fact that the relation between atmospheric parameters and module output maximum power is complex and non-linear, the use of artificial neural network-based models has been proposed. This approach has been followed by A.J. Rivera et al. [48]. In particular, a cooperative-competitive hybrid algorithm for radial basis function networks was implemented.

The model uses the Average Photon Energy (APE) [49,50] in order to quantify the spectral influences on HCPV module maximum power. This is a single value in eV that characterizes the shape of the spectrum, so that the higher APE, the higher the blue content of light. A spectroradiometer is required for obtaining this input.

The model takes into account the direct normal irradiance (DNI), the air temperature (T_{air}), the wind speed (WS) and the APE. Coefficients of the neural network are obtained from outdoor monitorized data.

4.5. Model of F. Almonacid et al. (2013)

The solar research group of Jaén University has wide experience on the application of artificial neural networks in the photovoltaic field [51–56]. Taking into account this experience and from a similar point of view than the previously commented model, the model proposed by F. Almonacid et al. [57] tries to characterize the relation between atmospheric parameters and module output maximum power through artificial neural networks. In this case, a feed-forward neural network trained with the Levenberg-Marquardt back-propagation algorithm was used.

The model takes into account the spectral influences through easily measurable parameters: air mass (AM) and precipitable water (PW). This way, it avoids the need of spectroradiometer. Inputs of the model are the direct normal irradiance (DNI), the air temperature (T_{air}), the wind speed (WS), the AM and the PW. Coefficients of the neural network are obtained from outdoor monitorized data.

Table 1
Comparison of characteristics of models for high concentration photovoltaic cells: required inputs and main advantages.

Models:	Equivalent circuit	Kinsey	Domínguez	Fernández	Sandia
Required inputs					
Concentration ratio	√	√	√	√	√
Cell temperature	√	√	√	√	√
Incident spectrum	√	√			
Subcells photocurrents			√	√	
Air mass					√
Advantages					
Provides the whole I-V curve	√		√	√	
Spectral effects quantified with high accuracy	√	√	√	√	
Explicit equations		√	√	√	√
Algorithms for extracting the model parameters are easy to implement		√		√	√
It does not require knowing in detail the incident spectrum			√	√	√
It does not require indoor characterization of the solar cell					√

4.6. Model of E.F. Fernández et al. (2012)

The model of E.F. Fernández et al. [35] uses air mass (AM) in order to quantify the spectral influences on HCPV module maximum power. Therefore, it avoids the need of spectroradiometer or isotype cells. The aim is to have a model based on easily measurable parameters. The main equations of the model are as follows:

$$P_{MPP} = A_1 \mathrm{DNI} + A_2 T_{air} \text{ for AM} \leq 2 \tag{17}$$

$$P_{MPP} = A_1 \mathrm{DNI} + A_2 T_{air} + A_3 \mathrm{AM} \text{ for AM} > 2 \tag{18}$$

These equations consider that, for large values of AM, P_{MPP} is mainly influenced by DNI, T_{air} and AM, while for small values of AM, the influence of AM can be neglected [58,59]. Coefficients A_1, A_2 and A_3 are obtained by regression analysis from outdoor monitorized data. At present, the model has been only evaluated at the south of Spain.

4.7. Model of Sandia National Laboratories (2004)

The models above only calculate the maximum power of the module. When more information about the device *I–V* curve is required, an alternative is to use the model of Sandia National Laboratories [36,60–63], which calculates five points of the *I–V* curve as shown in Fig. 4.

Equations of the model are formulated as a function of the "effective irradiance", which, for the case of a HCPV module, is defined as it is shown in Eq. (12).

The model equations that allow calculating the maximum power of a HCPV module are:

$$f_1(\mathrm{AM}) = a_0 + a_1 \mathrm{AM} + a_2 \mathrm{AM}^2 + a_3 \mathrm{AM}^3 + a_4 \mathrm{AM}^4 \tag{19}$$

$$B_{ef} = [\mathrm{DNI}\, f_1(\mathrm{AM})]/\mathrm{DNI}^* \tag{20}$$

$$\delta = [mk(T_C + 273.15)]/q \tag{21}$$

$$\beta_{Vmpp} = \beta_{Vmpp\,0} + m_{Vmpp}(1 - B_{ef}) \tag{22}$$

$$I_{MPP} = (C_0 B_{ef} + C_1 B_{ef}^2)[I^*_{MPP} + \alpha_{Impp}(T_C - T^*_C)] \tag{23}$$

$$V_{MPP} = V^*_{MPP} + C_2 N_S \delta \ln(B_{ef}) + C_3 N_S [\delta \ln(B_{ef})]^2 + \beta_{Vmpp}(T_C - T^*_C) \tag{24}$$

$$P_{MPP} = I_{MPP} V_{MPP} \tag{25}$$

Eq. (19) approximates the spectral correction factor, f_1(AM), as defined in the standard ASTM E 973 [40], by a fourth order polynomial. Eq. (20) calculates the effective irradiance (B_{ef}), that is, the irradiance at which the cells actually respond. This irradiance is the direct normal irradiance, DNI, corrected with the spectral correction factor, f_1(AM), and normalized to the reference irradiance, DNI*. Eq. (21) defines the δ parameter, which is the product of the effective ideality factor of the multi-junction cell (m) and the thermal voltage. The thermal voltage is obtained from the Boltzmann constant (k), the electron charge (q) and the cell temperature (T_C). Eq. (22) allows the determination of the temperature coefficient β_{Vmpp}. This coefficient is used afterwards for quantifying the effect of temperature on module maximum power point voltage. The coefficient is expressed as a linear function of the effective irradiance, i.e. it is allowed to vary with the concentration ratio. Eqs. (23) and (24) calculate the module maximum power point current (I_{MPP}) and voltage (V_{MPP}) from their values at reference conditions (I_{MPP}*, V_{MPP}*). The reference conditions are defined in the model by DNI*, T_C* and AM1.5. α_{Impp} is the temperature coefficient for I_{MPP} and N_S is the number of cells in series for the module. Finally, Eq. (25) obtains the maximum power of the HCPV module.

As it has been shown, some of the referenced module models use the mean cell temperature of the module (T_C) as input. The direct measurement of this parameter is very difficult, due to the special features of these kinds of devices. Because of this, indirect methods for estimating T_C have been proposed [42,64–69].

Table 2 summarizes the main characteristics of the referenced models for HCPV modules, including the required inputs and advantages of each one.

Table 3 presents a quantitative comparison of the referenced models for HCPV modules characterization. Four models have been evaluated at the Center of Advances Studies in Energy and Environment of Jaén University (ASTM E 2527, Almonacid, Fernández and Sandia). The rest of the models have been evaluated by their respective authors and results can be found in the papers that describe the models. With respect to the values shown in Table 3, it is important to remark that a direct comparison of the provided values is not possible because the different authors use different measurement and evaluation procedures. Furthermore,

Table 2
Comparison of characteristics of models for high concentration photovoltaic modules: required inputs and main advantages.

Models:	ASTM E 2527	Peharz	Steiner	Rivera	Almonacid	Fernández	Sandia
Required inputs							
Direct normal irradiance	√	√	√	√	√	√	√
Ambient temperature	√		√	√	√	√	
Wind speed	√		√	√	√		
Precipitable water			√		√		
Cell temperature		√					√
Incident spectrum			√				
Subcells photocurrents		√	√				
Average photon energy				√			
Aerosol optical depth			√				
Air mass					√	√	√
Tracking error			√				
Advantages							
It quantifies spectral effects		√	√	√	√	√	√
Spectral effects quantified with high accuracy		√	√	√			
It does not require the cell temperature	√		√	√	√	√	
It does not require spectroradiometer	√	√			√	√	√
It does not require indoor characterization	√			√	√	√	√
It provides electrical parameters other than P_{MPP}			√				√
Easy to implement	√	√				√	√
It does not require advanced knowledge on artificial neural networks	√	√	√			√	√
Low computational effort	√	√		√	√	√	√

Table 3
Errors between measured and calculated maximum power of the models for HCPV modules as provided by different authors.

Model	Parameter	Value
ASTM E 2527	RMSE	4.6%*
Peharz	Absolute RMSE	1.3, 1.2, 1.6 and 0.6 W**
Steiner	NRMSE	Between 2.5 and 3.2%***
Rivera	MSE	15.5****
Almonacid	RMSE	2.1%*
Fernández	RMSE	3.2%*
Sandia	RMSE	3.4%*

* Mean value of the root mean square error for two HCPV modules measured during 2011 and 2012 at the Center of Advanced Studies in Energy and Environment of Jaén University (south of Spain).

** Values of the absolute root mean square error for four HCPV modules measured in different time periods from 2009 to 2012 at the Fraunhofer ISE (Freiburg, Germany) [42]. The nominal power of the modules at 850 W/m^2 of direct normal irradiance, 25 °C of cell temperature under the incident spectrum AM 1.5d ASTM G173-03 is 54.0, 50.1, 44.0 and 15.7 W respectively.

*** Range of the obtained normalized root mean square error for five HCPV modules measured from November 2011 to March 2012 at the Fraunhofer ISE (Freiburg, Germany) [44]. The errors are normalized to the nominal power of each module.

**** Value of the mean square error for one HCPV module measured from November 2011 to March 2012 at Jaén University (south of Spain) [48].

the reported errors are expressed by different parameters in each case. However, the table can be illustrative of the order of magnitude of the errors of the models.

5. Conclusions

Nowadays, we can find in the scientific literature several models for the electrical characterization of HCPV cells and modules. These models are required for the design, monitoring and energy prediction of HCPV systems. A review of the existing models has been presented with the aim of helping the photovoltaic professionals and researchers in the choice of the most suitable model for each specific application.

Multijunction solar cell models calculate the relevant electrical parameters of the cell as a function of irradiance, spectrum and cell temperature. In order to evaluate the spectral influences, spectroradiometer, isotype cells or a solar simulator can be required. However, we can find other simplified models that require less sophisticated instruments in spite of a little loss of accuracy. Numerical algorithms are often needed in order to adjust the model parameters. These algorithms are not always easy to implement.

HCPV modules models calculate the relevant electrical parameters as a function of ambient parameters such as direct normal irradiance, air temperature or wind speed. The spectral influences can be characterized in different ways (Z, APE, AM) and different equipments are required to obtain these spectral parameters. Every model requires outdoor measurements in order to obtain the model coefficients by means of regression analysis. Some of these models are easy to implement and do not require very sophisticated instruments to be applied so that they are good candidates to be used in the industry, in particular the ASTM E 2527 [41], the model developed by Fernández et al. [35] and the model developed by Sandia National Laboratories [36].

Acknowledgments

This work is part of the project "SIGMPLANTAS: La innovación en las plantas y modelos de sistemas de Concentración Fotovoltaica en España", IPT-2011-1468-920000 supported by the Spanish Science and Innovation Ministry, and by the European Regional Development Fund/ Fondo Europeo de Desarrollo Regional (ERDF/ FEDER).

References

[1] Luque A, Andreev V, editors. Concentrator photovoltaics. Berlin, Heidelberg: Springer-Verlag; 2007.
[2] IEC 62108. Concentrator photovoltaic (CPV) modules and assemblies—design qualification and type approval. Edition 1.0. Geneve; 2007.
[3] Sala G, Pachón D, Antón I. Test, rating and specification of PV concentrator components and systems. C-rating project. Book 1: classification of PV concentrators. Contract NNE-1999-00588; 1999.
[4] Fraas L, Partain L. Solar cells and their applications. second edition. New Jersey: Wiley-Interscience; 2010.
[5] King RR, Fetzer CM, Edmondson KM, Law DC, Colter PC, Cotal HL et al. Metamorphic III–V materials, sublattice disorder, and multijunction solar cell approaches with over 37% efficiency. In: Proceedings of the European photovoltaic solar energy conference and exhibition; 2004.
[6] Dimroth F. High-efficiency solar cells from III–V compound semiconductors. Physica Status Solidi 2006;3:373–9.
[7] Law DC, King RR, Yoon H, Archer MJ, Boca A, Fetzer CM, et al. Future technology pathways of terrestrial III–V multijunction solar cells for concentrator photovoltaic systems. Solar Energy Materials and Solar Cells 2010;94:1314–8.
[8] Philipps SP, Peharz G, Hoheisel R, Hornung T, Al-Abbadi NM, Dimroth F, et al. Energy harvesting efficiency of III–V triple-junction concentrator solar cells under realistic spectral conditions. Solar Energy Materials and Solar Cells 2010;94:869–77.
[9] Pérez-Higueras PJ, Muñoz E, Almonacid G, Vidal PG. High concentrator photovoltaics efficiencies: present status and forecast. Renewable and Sustainable Energy Reviews 2011;15:1810–5.
[10] Green MA, Enery K, Hishikawa Y, Warta W, Dunlop ED. Solar cell efficiency tables (version 39). Progress in Photovoltaics: Research and Applications 2012;20:12–20.
[11] Emelyanov VM, Kalyuzhnyy NA, Mintairov MA, Mintairov SA, Shvartz MZ, Lantratov VM. Distributed resistance effects simulation in concentrator MJSCS using 3D-network model. In: Proceedings of the European solar energy conference and exibition, Valencia, Spain; 2010.
[12] Garcia I, Espinet-González P, Rey-Stolle I, Barrigón E, Algora C. Extended triple-junction solar cell 3D distributed model: application to chromatic aberration-related losses. In: Proceedings of the international conference on concentrating photovoltaic systems. CPV-7. AIP Conference Proceedings vol. 1407; 2011. p. 13–6.
[13] Wanlass MW, Emery KA, Gessert TA, Horner GS, Osterwald CR, Coutts TJ. Practical considerations in tandem cell modeling. Solar Cells 1989;27:191–204.
[14] Mittelman G. Cogeneration with concentrating photovoltaic systems. PhD Thesis. Tel Aviv University; 2006.
[15] Kribus A, Mittelman G. Practical cogeneration with concentrating PV. In: Proceedings of the international conference on concentrated solar concentrators for the generation of electricity or hydrogen (ICSC-4). El Escorial, Spain; 2007.
[16] Domínguez C, Antón I, Sala G. Multijunction solar cell model for translating I–V characteristics as a function of irradiance, spectrum and cell temperature. Progress in Photovoltaics: Research and Applications 2010;18:272–84.
[17] Segev G, Mittelman G, Kribus A. Equivalent circuit models for triple-junction concentrator solar cells. Solar Energy Materials and Solar Cells 2012;98:57–65.
[18] Ben Or A, Appelbaum J. Estimation of multi-junction solar cell parameters. Progress in Photovoltaics: Research and Applications 2013;21:713–23.
[19] Reinhardt KC, Mayberry CS, Lewis BP. Multijunction solar cell iso-junction dark current study. In: Proceedings of the Conference record of the ieee photovoltaic specialists conference; 2000. p. 1118–21.
[20] Nishioka K, Takamoto T, Agui T, Kaneiwa M, Uraoka Y, Fuyuki T. Evaluation of InGaP/InGaAs/Ge triple-junction solar cell under concentrated light by simulation program with integrated circuit emphasis. Japan Journal of Applied Physics 2004;43:882–9.
[21] Nishioka K, Sueto T, Uchina M, Ota Y. Detailed analysis of temperature characteristics of an InGaP/InGaAs/Ge triple-junction solar cell. Journal of Electronic Materials 2010;39:704–8.
[22] Heidler K, Raicu A, Wilson HR. A new approach for the performance evaluation of solar cells under realistic reporting conditions. In: Proceedings of the IEEE photovoltaic specialists conference, vol. 2; 1990. p. 1017–1022.
[23] Nann S, Emery K. Spectral effects on PV-device rating. Solar Energy Materials and Solar Cells 1992;27:189–216.
[24] Kinsey GS, Hebert P, Barbour KE, Krut DD, Cotal HL, Sherif RA. Concentrator multijunction solar cell characteristics under variable intensity and temperature. Progress in Photovoltaics: Research and Applications 2008;16:503–8.
[25] Kinsey GS, Edmondson KM. Spectral response and energy output of concentrator multijunction solar cells. Progress in Photovoltaics: Research and Applications 2009;17:279–88.
[26] Fernández EF, Siefer G, Schachtner M, García Loureiro AJ, Pérez-Higueras PJ. Temperature coefficients of monolithic III–V triple-junction solar cells under different spectra and irradiance levels. International conference on concentrating photovoltaic systems: CPV-8, AIP Conference Proceedings, vol. 1477; 2012. p. 189–93.

[27] Fernández EF, García-Loureiro AJ, Pérez-Higueras PJ, Siefer G. Monolithic III–V triple-junction solar cells under different temperatures and spectra Spanish Conference on Electron Devices CDE. Art. 5744222; 2011.
[28] Faine P, Kurtz SR, Riordan C, Olson JM. The influence of spectral solar irradiance variations on the performance of selected single-junction and multijunction solar cells. Solar Cells 1991;31:259–78.
[29] Siefer G, Bett AW. Analysis of temperature coefficients for III–V multi-junction concentrator cells. Progress in Photovoltaics: Research and Applications 2012. http://dx.doi.org/10.1002/pip.2285.
[30] ASTM E927-10. Standard specification for solar simulation for terrestrial photovoltaic testing. American Society for Testing and Materials.
[31] Spectrolab. 〈http://www.spectrolab.com/DataSheets/illumination/solarSim/T-HIPSS%20RevF.pdf〉 [accessed 1.02.13].
[32] Gueymard CA. Parameterized transmittance model for direct beam and circumsolar spectral irradiance. Solar Energy 2001;71:325–46.
[33] Gueymard CA. SMARTS2, a simple model of the atmospheric radiative transfer of sunshine: algorithms and performance assessment. Florida Solar Energy Center, Profesional Paper FSEC-PF-270-95; 1995.
[34] Fernández EF, Siefer G, Almonacid F, García Loureiro AJ, Pérez-Higueras PJ. A two subcell equivalent solar cell model for III–V triple junction solar cells under spectrum and temperature variations. Solar Energy 2013;92:221–9.
[35] Fernández EF. Modelización y caracterización de células solares III-V multiunión y de módulos de concentración. 2012 PhD thesis, Service of the University of Santiago de Compostela. 〈http://hdl.handle.net/10347/6156〉.
[36] King DL, Boyson WE, Kratochvil JA. Photovoltaic array performance model. Sandia National Laboratories, SAND2004-3535; 2004.
[37] Emery K, Delcueto J, Zaaiman W. Spectral corrections based on optical air mass. In: Proceedings of the IEEE photovoltaic specialists conference; 2002, p. 1725–8.
[38] Létay G, Baur C, Bett AW. Theoretical investigations of III–V multi-junction concentrator cells under realistic spectral conditions. In: Proceedings of the European photovoltaic solar energy conference; 2004.
[39] Kasten F, Young AT. Revised optical air mass tables and approximation formula. Applied Optics 1989;28:4735–8.
[40] ASTM E 973. Determination of the spectral mismatch parameter between a photovoltaic device and a photovoltaic reference cell. American Society for Testing and Materials; 2010.
[41] ASTM E 2527. Standard test method for electrical performance of concentrator terrestrial photovoltaic modules and systems under natural sunlight. American Society for Testing and Materials; 2009.
[42] Peharz G, Ferrer Rodríguez JP, Siefer G, Bett AW. A method for using CPV modules as temperature sensors and its application to rating procedures. Solar Energy Materials and Solar Cells 2011;95:2734–44.
[43] Peharz G, Siefer G, Bett AW. A simple method for quantifying spectral impacts on multi-junction solar cells. Solar Energy 2009;83:1588–98.
[44] Steiner M, Siefer G, Bösch A, Hornung T, Bett AW. Realistic power output modeling of CPV modules. In: Proceedings of the international conferencea on concentrating photovoltaic systems: CPV-8, AIP Conference Proceedings. vol. 1477; 2012 p. 309–12.
[45] Hornung T, Bachmaier A, Nitz P, Gombert A. Temperature dependent measurement and simulation of Fresnel lenses for concentrating photovoltaics. In: Proceedings of the international conference on concentrating photovoltaic systems: CPV-6, AIP Conference Proceedings , vol 1277; 2010 p. 85–8.
[46] LTSpice. Switcher CAD III/LT spice. 〈http://www.linear.com/designtools/software〉[accessed 1.02.13].
[47] Steiner M, Guter W, Peharz G, Philipps SP, Dimroth F, Bett AW. A validated SPICE network simulation study on improving tunnel diodes by introducing lateral conduction layers. Progress in Photovoltaics: Research and Applications 2012;20:274–83.
[48] Rivera AJ, García-Domingo B, del Jesús MJ, Aguilera J. Characterization of concentrating photovoltaic modules by cooperative competitive radial basis function networks. Expert Systems with Applications 2013;40:1599–608.
[49] Williams S, Betts T, Helf T, Gottschalg R, Beyer H. Infield D. Modeling long term module performance based on realistic reporting conditions with consideration to spectral effects. In: Proceedings of the world conference on photovoltaic energy conversion Vol. B; 2003.
[50] Minemoto T, Nakada Y, Takahashi H, Takakura H. Uniqueness verification of solar spectrum index of average photon energy for evaluating outdoor performance of photovoltaic modules. Solar Energy 2009;83:1294–9.
[51] Almonacid F, Hontoria L, Rus C, Fuentes M, Nofuentes G. Characterisation of PV modules using artificial neural network. Renewable Energy 2009;34:941–4.
[52] Almonacid F, Rus C, Hontoria L, Muñoz FJ. Characterisation of PV CIS module by artificial neural networks, a comparative study with other methods. Renewable Energy 2010;35:973–80.
[53] Almonacid F, Rus C, Pérez-Higueras PJ, Hontoria L. Estimation of the energy of a PV generator using artificial neural network. Renewable Energy 2009;34:2743–50.
[54] Almonacid F, Rus C, Pérez-Higueras PJ, Hontoria L. Calculation of the energy provided by a PV generator. Comparative study: conventional methods vs. artificial neural networks. Energy 2011;36:375–84.
[55] Almonacid F, Pérez-Higueras PJ, Rodrigo P, Hontoria L. Generation of ambient temperature hourly time series for some Spanish locations by artificial neural networks. Renewable Energy 2013;51:285–91.
[56] Rodrigo P, Rus C, Almonacid F, Pérez-Higueras PJ, Almonacid G. A new method for estimating angular, spectral and low irradiance losses in photovoltaic systems using an artificial neural network model in combination with the Osterwald model. Solar Energy Materials and Solar Cells 2012;96:186–94.
[57] Almonacid F, Fernández EF, Pérez-Higueras PJ, Rodrigo P, Rus-Casas C. Estimating the maximum power of a High Concentrator Photovoltaic (HCPV) module using an artificial neural network. Energy 2013;53:165–72.
[58] Fernández EF, Pérez-Higueras PJ, García-Loureiro AJ, Vidal PG. Outdoor evaluation of concentrator photovoltaic systems modules from different manufacturers: first results and steps. Progress in Photovoltaics: Research and Applications 2013;21:693–701.
[59] Fernández EF, Pérez-Higueras PJ, Almonacid F, García-Loureiro AJ, Fernández JI, Rodrigo P, et al. Quantifying the effect of air temperature in CPV modules under outdoor conditions. In: Proceedings of the 8th international conference on concentrating photovoltaic systems, AIP Conference Proceedings, vol. 1477; 2012, p. 194–7.
[60] King DL. Photovoltaic module and array performance characterization methods for all system operating conditions. NREL/SNL Photovoltaics Program Review Meeting; 1997.
[61] King DL, Kratochvil JA. Temperature coefficients for PV modules and arrays: measurement methods, difficulties and results. In: Proceedings of the IEEE photovoltaic specialists conference; 1997.
[62] King DL, Kratochvil JA. Measuring solar spectral and angle-of-incidence effects on photovoltaic modules and solar irradiance sensors. In: Proceedings of the IEEE photovoltaic specialists conference; 1997.
[63] King DL, Kratochvil JA, Boyson WE, Bower WI. Field experience with a new performance characterization procedure for photovoltaic arrays. In: Proceedings of the world conference and exhibition on photovoltaic solar energy conversion; 1998.
[64] ISFOC. Specifications of general conditions for the call for tenders for concentration photovoltaic solar plants for the Institute of Concentration Photovoltaic Systems; 2007.
[65] Rubio F, Martínez M, Coronado R, Pachón JL, Banda P. Deploying HCPV power plant – ISFOC experiences. In: Proceedings of the IEEE photovoltaic specialists conference, vol. 387; 2008, p. 381–4.
[66] Almonacid F, Pérez-Higueras PJ, Fernández EF, Rodrigo P. Relation between the cell temperature of a HCPV module and atmospheric parameters. Solar Energy Materials and Solar Cells 2012;105:322–7.
[67] Jaus J, Peharz G, Gombert A, Ferrer Rodríguez JP, Dimroth F, Eltermann F et al. Development of FLATCON® modules using secondary optics. In: Proceedings of the IEEE Photovoltaic Specialist Conference; 2009 p. 1931–6.
[68] Kemmoku Y, Egami T, Hiramatsu M, Miyazaki Y, Araki K, Ekins-Daukes NJ et al. Modeling of module temperature of a concentrator PV system. In: Proceedings of the European photovoltaic solar energy conference; 2004.
[69] Fernández EF, García Loureiro AJ, Rodrigo P, Almonacid F, Fernández JI, Pérez-Higueras PJ, et al. Calculation of cell temperature in a HCPV module using Voc. Spanish Conference on Electron Devices CDE 2013; 317-20.